Thermoresponsive Nanocellulose Hydrogels with Tunable Mechanical Properties

Jason R. McKee,[†] Sami Hietala,[‡] Jani Seitsonen,[§] Janne Laine,[||] Eero Kontturi,*[,||] and Olli Ikkala*[,†]

[†]Molecular Materials, Department of Applied Physics and [§]Nanomicroscopy Center, Aalto University, P.O. Box 15100, FIN-00076 Aalto, Espoo, Finland

[‡]Laboratory of Polymer Chemistry, Department of Chemistry, University of Helsinki, P.O. Box 55, FIN-00014 HY, Helsinki, Finland

[||]Department of Forest Products Technology, Aalto University, P.O. Box 16300, FIN-00076 Aalto, Espoo, Finland

ⓢ *Supporting Information*

ABSTRACT: Cellulose microfibrils physically bound together by soft hemicellulose chains form the scaffolding that makes plant cell walls strong. Inspired by this architecture, we designed biomimetic thermoreversible hydrogel networks based on reinforcing cellulose nanocrystals (CNC) and thermoresponsive methylcellulose (MC). Upon dissolving MC powder in CNC aqueous dispersions, viscoelastic dispersions were formed at 20 °C, where the storage modulus (G') is tunable from 1.0 to 75 Pa upon increasing the CNC concentration from 0 to 3.5 wt % with 1.0 wt % MC. By contrast, at 60 °C a distinct gel state is obtained with $G' \gg G''$, $G' \sim \omega^0$, with an order of magnitude larger G' values from 110 to 900 Pa upon increasing the CNC concentration from 0 to 3.5 wt % with constant 1.0 wt % MC, due to the physical cross-links between MC and CNCs. Therefore, simply mixing two sustainable components leads to the first all-cellulose thermoreversible and tunable nanocellulose-based hydrogels.
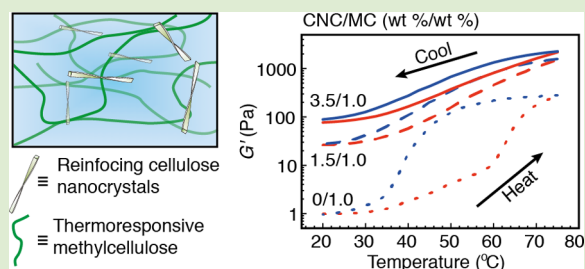
Over the years, a wide range of materials have been pursued with engineered responsive or switchable functional properties based on structures that respond to imposed conditions or stimuli. Common approaches have been, for example, to combine stimulus adaptability with self-assembled structures, wetting of surfaces or interfaces, or percolation or swelling of networks and gels.[1−9] Perhaps the most straightforward external stimulus is temperature. In this regard, synthetic thermoresponsive polymers, such as aqueous solutions of poly(N-isopropyl acrylamide) or poly(N-vinyl caprolactam), undergo a coil-to-globule transition upon heating past their respective cloud points allowing for thermoresponsive hydrogels.[8] Therein, upon heating the polymer–water hydrogen bonds gradually dissociate and water forms internal clathrate structures. Temperature has been widely used as a stimulus for biomedical applications, such as for drug release and responsive scaffolds for regenerative medicine.[6,8,9]

On the other hand, biological materials and their multifunctional structures have attracted considerable attention as they offer examples for excellent mechanical properties using sustainable starting materials.[10] Natural materials typically involve subtle combinations of self-assemblies or networks at different length scales with reinforcing hard phases and soft phases, with examples found in the nanostructure of plant cell walls, silk and exoskeletons of various organisms. However, biological materials have remained challenging to scale up for technological applications. Therein, biomimetics aims to identify and exploit the most essential aspects of biological materials in technologically feasible ways.[11−14] For example, the structure of plant cell walls consists of mechanically strong reinforcing microfibrillated native cellulose nanofibers connected by soft polymeric hemicellulose chains that physically bind the fibril assemblies together to form mechanically strong networks (Figure S1).[15] Inspired by such nanocomposite structures, our aim here was to construct biomimetic hydrogels consisting of hard reinforcing colloidal nanocellulose rods physically connected by soft thermoresponsive cellulose derivatives. By this combination we aim to create thermoresponsive and tunable all-cellulose bionanocomposite hydrogels with both enhanced and stimulus responsive mechanical properties, which has not been previously reported.

Recently several techniques have been provided to extract nanosized cellulose from plant cell walls, either as long and entangled nanofibrillated cellulose or short rod-like cellulose nanocrystals.[16−19] Both types of nanocellulose have diameters of a few nanometers and high mechanical properties, with a modulus value in the order of about 140 GPa and a tensile strength in the GPa range due to the highly hydrogen-bonded assembly of parallel cellulose chains in their native cellulose I crystalline domains.[20,21] Here we investigated cellulose nanocrystals (CNC) as they contain anionic sulfate ester groups which allow electrostatic colloidal stabilization in water. Indeed, even at high concentrations (3.7 wt %), CNCs behave as free-flowing colloidal dispersions (see Figures S2c and S3) unlike
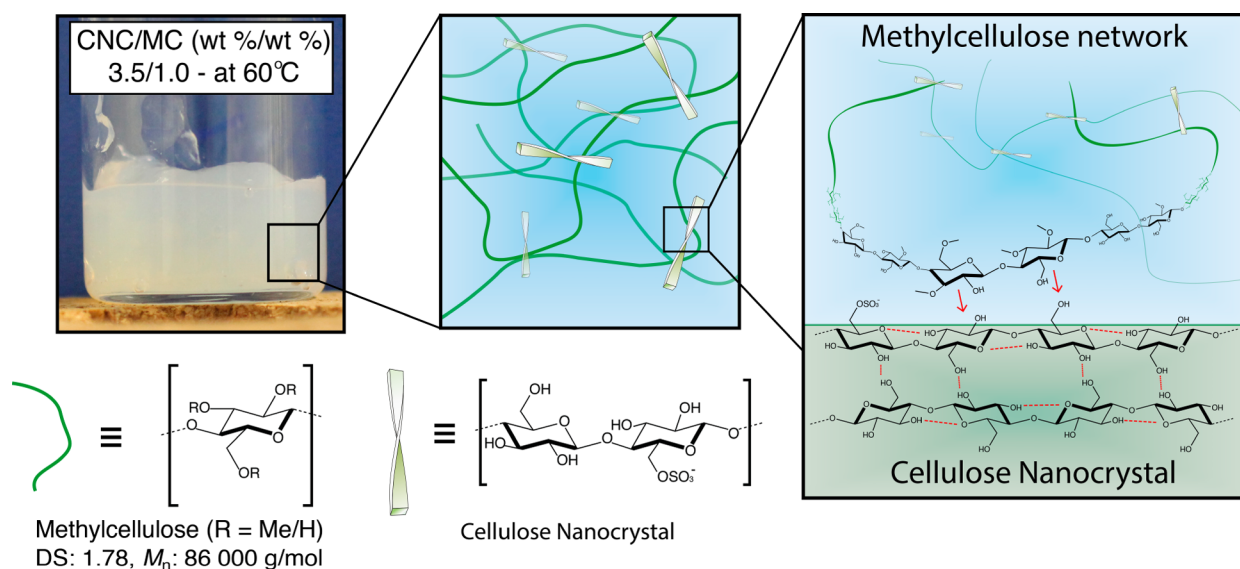
Figure 1. Photograph showing gelation as seen from the sample CNC/MC 3.5 wt %/1.0 wt % at 60 °C. Here, MC has a M_n of 86000 g/mol and a DS of 1.78. Also included is a schematic representation of the nanocomposite hydrogel. The suggested adsorption of MC on CNC is indicated by red arrows.
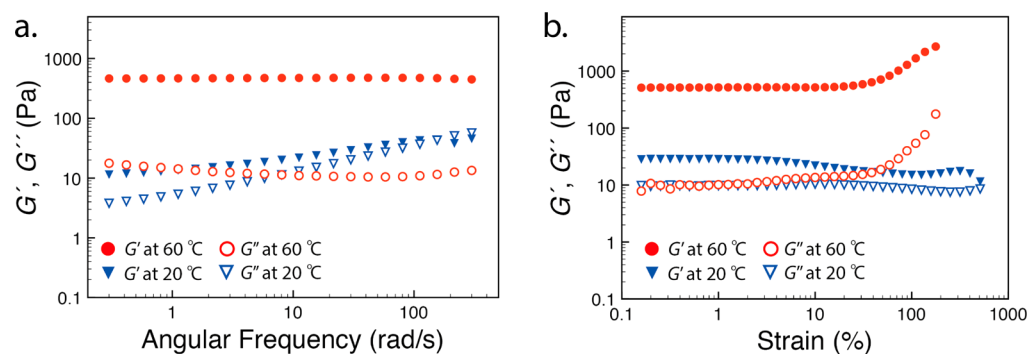

Figure 2. Typical oscillatory rheological behavior, as shown by the nanocomposite hydrogel with a 1.5 wt % cellulose nanocrystal (CNC) and 1.0 wt % methyl cellulose (MC) loading: (a) frequency sweep preformed between 0.1−300 rad/s at 60 °C (red) and 20 °C (blue), determined at 10% strain; (b) strain sweeps at 60 °C (red) and 20 °C (blue), determined at an angular frequency of 6.283 rad/s. The linear low strain G' value was ca. 510 Pa at 60 °C.

nanofibrillated cellulose (NFC), which form hydrogels even at low concentrations (∼1 wt %). Hence, mixing polymers with NFC requires a lot of energy, which is a major drawback for scalability. CNCs have been widely used in materials science, for example, to imbue CNCs' chiral assemblies into optical functions, healable materials, or to embed CNCs in matrix polymers for nanoreinforcement.[22−26] In this regard, CNCs are suitable candidates for the present architecture.

For the soft binding polymer, we selected methylcellulose (MC) as it is a widely available nontoxic commercial cellulose derivative that undergoes thermoreversible gelation in aqueous solutions.[27−31] This reversible transition has recently attracted considerable interest.[30,31] Depending on the degree of methoxy substitution (generally the degree of substitution DS ∼ 1.6−2.1), heating rate, and aqueous concentration, the thermal transition generally resides in the range 50−60 °C.[30,31] It has been suggested that the gelation mechanism occurs via nucleation and growth, as the heating rate has been shown to have a strong effect on the transition temperature.[31] Upon heating, the network undergoes a drastic change where the single MC strands lose part of their affinity to the surrounding water and subsequently start to bundle up into about 14 nm

thick fibrils.[30,32,33] This fibrillation is observed as a sol-to-gel transition with considerably increased storage modulus (G') values as well as an increase in turbidity.[31] For the present work, an important aspect of MC and several other cellulose derivatives is that they bind with cellulose surfaces.[34,35] Therefore, a composite gel network between CNCs and MC is foreseen, where the rod-like CNCs are expected to physically cross-link the MC network, which would lead to tunable moduli.

In this regard, we explored aqueous dispersions consisting of both hard reinforcing CNC colloidal rods and soft MC polymer chains to create physically bound nanocomposite networks (see Figure 1 for the components). The CNCs were extracted from cotton filter paper by sulfuric acid hydrolysis,[36] resulting in crystalline nanoscale rods of lateral diameter a few nanometers and lengths ranging from 50 to 300 nm. The surface is dotted with a set of anionic sulfate ester groups to prevent the intrinsic self-aggregation in aqueous suspensions. The commercially available MC used here had a number averaged molecular weight (M_n) of 86000 g/mol and an average degree of methoxy substitution (DS) of 1.78. A series of nanocomposite compositions were fabricated by systematically increasing the
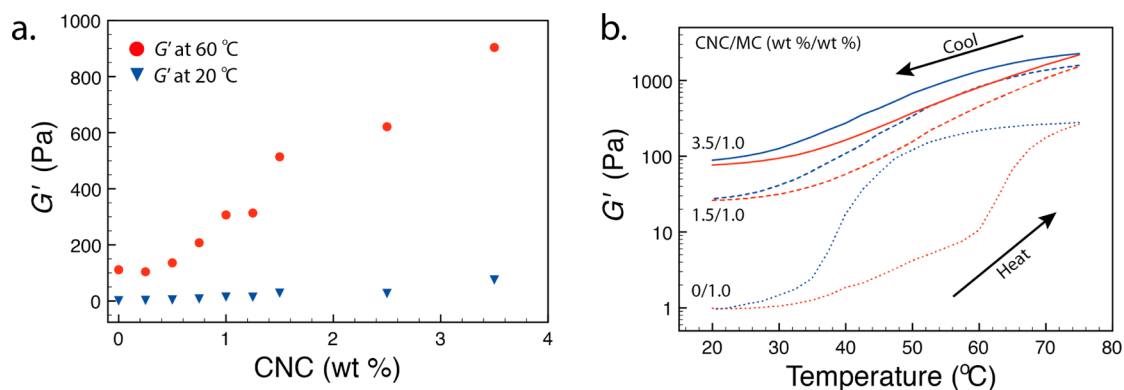
Figure 3. (a) Low strain limit G' values for hydrogels with increasing cellulose nanocrystal (CNC) loadings at 60 °C (red) and 20 °C (blue) while keeping a fixed amount 1 wt % of methyl cellulose (MC), as determined via strain sweeps at an angular frequency of 6.283 rad/s. (b) Cyclic heating of the samples with 0, 1.5, and 3.5 wt % CNC loading while keeping a fixed amount 1 wt % of methyl cellulose (MC), where G' was determined at an angular frequency of 6.283 rad/s and 2.0% strain. The temperature was increased and decreased at 2.5 °C intervals during which the sample was equilibrated for 45 s.

amount of CNCs from 0 to 3.5 wt % with a fixed amount 1.0 wt % of MC (Table S1) by dissolving dry MC powder into CNC aqueous dispersions, followed by mechanical stirring at room temperature (21 °C).

Depending on the temperature and CNC loading, the aqueous CNC/MC mixtures showed two types of behavior. At 20 °C, a visual inspection showed that they were viscous dispersions qualitatively demonstrating higher viscosity upon increasing the CNC concentration, and finally gel-like properties for the sample CNC/MC 3.5 wt %/1.0 wt % involving the highest studied CNC fraction. Systematic rheological measurements were performed at 20 °C by increasing the amount of CNCs while keeping a fixed MC amount of 1.0 wt % (Figure S4). With low CNC loadings (up to ca. 0.25 wt % CNC), the overall behavior remained reminiscent of viscous liquids at 20 °C where the loss modulus G'' dominated over G'. At higher CNC loadings (>0.5 wt % CNC), the storage modulus (G') gradually started to dominate, such as in the case CNC/MC 1.5 wt %/1.0 wt % (Figure 2a) and at even higher CNC concentrations (Figure S4). The strain sweeps demonstrated linear viscoelastic regions up to around 10% strain at 20 °C. Beyond this, the material demonstrated some shear thinning with slight decrease in the G' values (Figures 2b and S4). With increasing CNC loading, the low strain limit G' value increased from 1.0 Pa, without CNC, to 75 Pa for the sample that contained 3.5 wt % CNC. This indicates reinforcing effect of CNCs within the compositions. It could therefore be concluded that, at room temperature, the addition of CNCs increases the storage modulus and viscosity, resulting in gelation at high enough CNC concentrations.

However, a distinct change was observed by heating the CNC/MC aqueous mixtures to 60°C (Figures 2 and S4). Figure 1 shows a photograph of a turbid gel of CNC/MC 3.5 wt %/1.0 wt % at 60 °C (see also Figure S2a). Rheology showed that $G' \sim \omega^0$ and $G' \gg G''$ in all compositions, characteristic for elastic gels (Figures 2a and S4). The low strain limit G' values demonstrated a near-linear increase from 0.25 to 3.5 wt % CNC loading (Figure 3a and Table S1). By comparing the reference sample of pure MC to the sample CNC/MC 3.5 wt %/1.0 wt %, roughly 1 order of magnitude increase in the low strain G' value was observed at 60 °C, thus showing the tunability of the gel modulus upon adding CNCs. Strain hardening was also observed in each CNC/MC gel at 60 °C, as

seen from the strain sweeps beyond roughly 30−50% strain up to 200−300% strain (Figures 2b and S4). Finally, at very high strains the measurements became unreliable due to the plate slippage.

The above observations can be compared to pure components. Pristine CNCs at 3.7 wt % showed no gelation (Figure S3), as expected. The reference sample of pure MC at 1.0 wt % also behaved as expected: it was a viscous fluid at 20 °C with G'' dominating over most of the studied frequency range and a clear sol−gel transition occurring when the temperature was raised to 60 °C (Figure S4a). At 60 °C, G' started to dominate over G'' across the whole frequency range. Moreover, at 60 °C the strain sweep demonstrated a broad linear elastic range up to about 20% strain, after which strain hardening was observed upon approaching 400% strain. Although starker contrasts versus the room temperature behavior could have been observed with even higher temperatures, we realized that, for example, at 70 °C the evaporation of water started to interfere excessively with the reproducibility of more time-consuming measurements, such as broad frequency sweeps. The thermoresponsive behavior of MC between 20 and 60 °C was similar to the previously reported results.[31] Thus, in comparison to the component materials, the mixtures CNC/MC allow to tune both the room temperature dispersion viscosity as well as the high temperature nanocomposite hydrogel moduli.

The reversibility of the thermal transition was inspected more closely by imposing heating/cooling cycles from 20 to 75 °C and back to 20 °C where G' and G'' were measured using fixed frequency and strain values. Figure 3b shows G' as a function of temperature for the samples that contained 0, 1.5, and 3.5 wt % CNC loading, each containing 1.0 wt % MC (Figure S5 shows additionally the behavior of G''). According to the cyclic measurements, each material recovered its original G', indicating a fully thermoreversible transition. The 1.0 wt % MC reference sample behaved as previously observed: large hysteresis in the heating and cooling cycle and a time-dependent transition.[30,31] With added CNCs, however, the hysteresis became markedly smaller, possibly due to the highly hydrophilic CNCs allowing the MC chains to hydrate faster during cooling due to their interaction. At 75 °C, the 1.0 wt % MC reference had a G' value of 270 Pa, whereas adding 1.5 and 3.5 wt % CNC loading increased the low strain G' values to

1500 and 2200 Pa, respectively, indicating efficient reinforcement of MC networks by CNCs up to 75 °C.

Our initial hypothesis was that adding CNCs leads to an overall increase in the number of physical cross-links within the MC network in the gel state, which would result in higher G' values when compared to the 1.0 wt % MC reference sample. This assumption was supported by comparing the G' values of two nanocomposite samples (1.5 and 3.5 wt % CNC loading and 1.0 wt % MC) at 60 and 75 °C to the relative modulus increase against the pure MC reference (Table S2, Figure 3). According to these results, the relative modulus increase did not change significantly between these temperatures, suggesting that the relative increase in the modulus values versus the MC reference resulted from the physical cross-links, whereas the increase in modulus versus temperature resulted mainly from the MC.

Finally, cryo-TEM images of the nanocomposite gels were used to determine how well the CNCs had dispersed within the MC-component. Hydrogel samples at specific CNC concentrations (see SI for further information) were blotted and subsequently flash-frozen from 20 °C (Figures 4 and S6). As
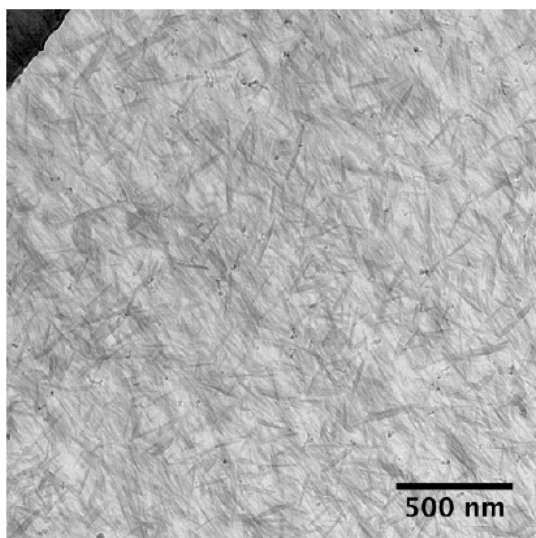

Figure 4. Cryo-TEM image flash-frozen after annealing at 20 °C for the sample with 0.5 wt % CNC and 1 wt % MC loading. Note the well-dispersed CNCs.

expected, each sample demonstrated that the CNCs had indeed been embedded homogeneously within the MC matrix without any apparent aggregation. This indicates that both components were also fully compatible in the nanoscale.

To conclude, we have herein demonstrated a particularly facile and scalable fabrication process for tunable biobased all-cellulose thermoresponsive gels incorporating a mixture of colloidal rod-like cellulose nanocrystals physically bound together by methylcellulose. At 20 °C, the CNC/MC systems behaved as viscous dispersions with low CNC loading. By further increasing the CNC concentration, the systems' modulus increased until finally a weak gel was observed with a 3.5 wt % CNC loading. When heated to 60 °C, the G' values increased by 1 order of magnitude and the samples behaved as distinct gels $G' \sim \omega^0$ and $G' \gg G''$. Thus, by changing the CNC loading and temperature, the storage modulus values of the nanocomposite hydrogels could be tuned over a broad window of 3 orders of magnitude: from 1 Pa (20 °C) to 2200

Pa (75 °C) with a fixed amount of methylcellulose (1.0 wt %). This facile method allows for good homogeneous dispersion of CNCs within a biopolymer matrix and paves way for new types of CNC-based hydrogel materials.

ASSOCIATED CONTENT

ⓢ Supporting Information
Detailed information on the fabrication process, rheological characterization, and additional cryo-TEM images. This material is available free of charge via the Internet at http://pubs.acs.org.

AUTHOR INFORMATION

Corresponding Authors
*E-mail: olli.ikkala@aalto.fi.
*E-mail: eero.kontturi@aalto.fi.

Notes
The authors declare no competing financial interest.

REFERENCES
(1) Ozin, G. A.; Arsenault, A. C. *Nanochemistry; A Chemical Approach to Nanomaterials*; RSC Publishing: Cambridge, 2005.
(2) Kang, Y.; Walish, J. J.; Gorishnyy, T.; Thomas, E. L. *Nat. Mater.* **2007**, *6*, 957.
(3) ten Brinke, G.; Ruokolainen, J.; Ikkala, O. *Adv. Polym. Sci.* **2007**, *207*, 113.
(4) Capadona, J. R.; Shanmuganathan, K.; Tyler, D. J.; Rowan, S. J.; Weder, C. *Science* **2008**, *319*, 1370.
(5) Lyon, L. A.; Meng, Z.; Singh, N.; Sorrell, C. D.; St. John, A. *Chem. Soc. Rev.* **2009**, *38*, 865.
(6) Stuart Cohen, M. A.; Huck, W. T. S.; Genzer, J.; Müller, M.; Ober, C.; Stamm, M.; Sukhorukov, G. B.; Szleifer, I.; Tsukruk, V. V.; Urban, M.; Winnik, F.; Zauscher, S.; Luzinov, I.; Minko, S. *Nat. Mater.* **2010**, *9*, 101.
(7) Vlassopoulos, D.; Fytas, G. *Adv. Polym. Sci.* **2010**, *236*, 1.
(8) Aseyev, V.; Tenhu, H.; Winnik, F. M. *Adv. Polym. Sci.* **2011**, *242*, 29.
(9) Yamato, M.; Akiyama, Y.; Kobayashi, J.; Yang, J.; Kikuchi, A.; Okano, T. *Prog. Polym. Sci.* **2007**, *32*, 1123.
(10) Meyers, M. A.; Chen, P. Y.; Lin, A. Y. M.; Seki, Y. *Prog. Mater. Sci.* **2008**, *53*, 1.
(11) Fratzl, P.; Weinkamer, R. *Prog. Mater. Sci* **2007**, *52*, 1263.
(12) Bhushan, B. *Philos. Trans. R. Soc., A* **2009**, *367*, 1445.
(13) Espinosa, H. D.; Rim, J. E.; Barthelat, F.; Buehler, M. J. *Prog. Mater. Sci* **2009**, *54*, 1059.
(14) Stone, D. A.; Korley, L. T. J. *Macromolecules* **2010**, *43*, 9217.
(15) Cosgrove, D. J. *Nat. Mol. Cell Biol.* **2005**, *6*, 850.
(16) Moon, R. J.; Ashlie, M.; Nairn, J.; Simonsen, J.; Youngblood, J. *Chem. Soc. Rev.* **2011**, *40*, 3941.
(17) Klemm, D.; Kramer, F.; Moritz, S.; Lindström, T.; Ankerfors, M.; Gray, D.; Dorris, A. *Angew. Chem., Int. Ed.* **2011**, *50*, 5438.
(18) Eichhorn, S. J. *Soft Matter* **2011**, *7*, 303.
(19) Habibi, Y.; Lucia, L. A.; Rojas, O. J. *Chem. Rev.* **2010**, *110*, 3479.
(20) Saito, T.; Kimura, S.; Nishiyama, Y.; Isogai, A. *Biomacromolecules* **2007**, *8*, 2485.
(21) Saito, T.; Kuramae, R.; Wohlert, J.; Berglund, L. A.; Isogai, A. *Biomacromolecules* **2013**, *14*, 248.
(22) Fleming, K.; Gray, D. G.; Matthews, S. *Chem.—Eur. J.* **2001**, *7*, 1831.

(23) Kelly, J. A.; Shukaliak, A. M.; Cheung, C. C. Y.; Shopsowitz, K. E.; Hamad, W. Y.; MacLachlan, M. J. *Angew. Chem., Int. Ed.* **2013**, *52*, 8912.

(24) Lin, N.; Huang, J.; Dufresne, A. *Nanoscale* **2012**, *4*, 3274.

(25) Fox, J.; Wie, J. J.; Greenland, B. W.; Burattini, S.; Hayes, W.; Colquhoun, H. M.; Mackay, M. E.; Rowan, S. J. *J. Am. Chem. Soc.* **2012**, *134*, 5362.

(26) Shanmuganathan, K.; Capadona, J. R.; Rowan, S. J.; Weder, C. *Prog. Polym. Sci.* **2010**, *35*, 212.

(27) Kato, T.; Yokoyama, M.; Takahashi, A. *Colloid Polym. Sci.* **1978**, *256*, 15.

(28) Desbrières, J.; Hirrien, M.; Ross-Murphy, S. B. *Polymer* **2000**, *41*, 2451.

(29) Kobayashi, K.; Huang, C.-i.; Lodge, T. P. *Macromolecules* **1999**, *32*, 7070.

(30) Lott, J. R.; McAllister, J. W.; Arvidson, S. A.; Bates, F. S.; Lodge, T. P. *Biomacromolecules* **2013**, *14*, 2484.

(31) Arvidson, S. A.; Lott, J. R.; McAllister, J. W.; Zhang, J.; Bates, F. S.; Lodge, T. P.; Sammler, R. L.; Li, Y.; Brackhagen, M. *Macromolecules* **2013**, *46*, 300.

(32) Bodvik, R.; Dedinaite, A.; Karlson, L.; Bergström, M.; Bäverbäck, P.; Pedersen, J. S.; Edwards, K.; Karlsson, G.; Varga, I.; Claesson, P. M. *Colloids Surf., A* **2010**, *354*, 162.

(33) Bodvik, R.; Karlson, L.; Edwards, K.; Eriksson, J.; Thormann, E.; Claesson, P. M. *Langmuir* **2012**, *28*, 13562.

(34) Kondo, T. *J. Polym. Sci., Part B: Polym. Phys.* **1997**, *35*, 717.

(35) Yang, X.; Bakaic, E.; Hoare, T.; Cranston, E. D. *Biomacromolecules* **2013**, *14*, 4447.

(36) Edgar, C. D.; Gray, D. G. *Cellulose* **2003**, *10*, 299.